Current Medical Imaging, 2021, *17*, 342-351

RESEARCH ARTICLE

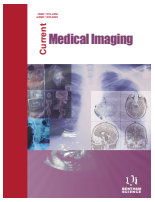

The Learning-based Automatic Segmentation Algorithm of Brain MR Images Based on 7T

Minghui Deng[1,*], Jin Zhenhao[1], Ran Yu[1] and Qingshuang Zeng[2]

[1]*College of Electrical and Information, Northeast Agricultural University, Changjiang Road 600, Harbin, China;* [2]*School of Astronautics, Harin Institute of Technology, West Direct Street 92, Harbin, China*

Abstract: ***Background*:** The learning-based algorithms provide an ability to automatically estimate and refine GM, WM and CSF. The ground truth manually achieved from the 3T MR image may not be accurate and reliable with poor image intensity contrast. It will seriously influence the classification performance because the supervised learning-based algorithms extremely rely on the ground truth. Recently, the 7T MR images brings about the excellent image intensity contrast, while Structured Random Forest (SRF) performs the pixel-level classification and achieves structural and contextual information in images.

***Materials and Methods*:** In this paper, a automatic segmentation algorithm is proposed based on ground truth achieved by the corresponding 7T subjects for segmenting the 3T&1.5T brain tissues using SRF classifiers. Through taking advantage of the 7T brain MR images, we can achieve the highly accuracy and reliable ground truth and then implement the training of SRF classifiers. Our proposed algorithm effectively integrates the T1-weighed images along with the probability maps to train the SRF classifiers for brain tissue segmentation.

***Results*:** Specifically, for the mean Dice ratio of all 10 subjects, the proposed method achieved 95.14%±0.9%, 90.17%±1.83%, and 81.96%±4.32% for WM, GM, and CSF. With the experiment results, the proposed algorithm can achieve better performances than other automatic segmentation methods. Further experiments are performed on the 200 3T&1.5T brain MR images of ADNI dataset and our proposed method shows promised performances.

***Conclusion*:** The authors have developed and validated a novel fully automated method for 3T brain MR image segmentation.

ARTICLE HISTORY

Received: December 01, 2019
Revised: May 18, 2020
Accepted: June 08, 2020

DOI:
10.2174/1573405616666200806171509

Keywords: Magnetic resonance imaging, machine learning, structured random forest, image processing, cerebral tissues, principal components analysis.

1. INTRODUCTION

Magnetic Resonance Imaging (MRI) is very important and indispensable for diagnosis and study of brain illnesses. Based on the MRI technique, the study of brain MRI generally requires a segmentation step on the main cerebral tissues [1]. The segmentation of brain images is of practical value and useful in clinical diagnosis and treatment of brain illnesses [2]. In MRI data analysis, although many algorithms designed to achieve the precise segmentation of different brain tissues for brain studies have been reported, automatic segmentation still is very difficult [3].

There are many learning-based algorithms to analyze MR images, including support vector machines(SVM) [4, 5], principal components analysis (PCA) [6], K-Nearest Neighbor (KNN) [7] and deep convolutional neural networks (CNN) [8]. Recently, the segmentation algorithm with random decision forest is excellent for large-scale image data [9]. The research on the automatic learning-based methods of brain MR image segmentation based on the random forest is very popular [10-13]. Few learning-based automatic segmentation methods have proven to be effective for all situations. How to overcome the unreliability and inaccuracy of ground truth obtained from the 3T brain MR images is very challenging for the learning-based algorithm on brain MR image.

The investigation about 7T shows significantly higher sensitivity [14]. During the last few years, 7T shows higher intensity contrast [15-17]. Thus, 7T has been considered as an excellent imaging and providing better resolved anatomical details than conventional MRI [18]. But at present, most MR systems used for clinical patients are 1.5T or 3T systems. How to take advantage of the combination of 3T and 7T for the clinical investigation is still unexplored.

* Address correspondence to this author at the College of Electrical and Information, Northeast Agricultural University, Changjiang Road 600, Harbin, China; E-mail: markdmh@163.com

1875-6603/21 $65.00+.00

In this article, a learning-based segmentation algorithm on brain MR images with Structured Random Forest theory is especially presented. We improve the LINKS scheme, which has been recently proposed for accurate tissue segmentation on infant brain MR images by integrating multi--source images information together. The structured random forest technique is employed in the LINKS scheme for brain segmentation [13]. We train a cascade of multi-class Structured Random Forest classifiers based on training data consisting of 3T T1-weighted images and segmentation labels from 7T T1-weighted images. On the base of the excellent intensity contrast of 7T brain MR images, we can directly and accurately attain the ground truth for our learning-based method. To address this issue, the whole hemisphere segmentation analysis of ground truth was conducted using 7T and the comparison to the 3T standard was carried out to assess accuracy and reliability for each region. In the application stage, given an unseen MR image, the learned classifiers are sequentially applied to progressively refine the tissue probability maps for achieving final tissue segmentation.

2. METHODS

2.1. Data Acquisition and Image Processing

This study was approved by the Institutional Review Board (IRB) of the Northeast Agricultural University and written informed consent forms were obtained from all subjects. A total of 10 volunteers (4 males and 6 females) with the age of 28±6 yr were recruited for this study. We have 10 training subjects of T1 brain images. All the 7T MR images were achieved with 7T Siemens MRI scanner. The 7T T1-weighted MR images were acquired with 192 sagittal slices using two sets of parameters: (1) 300 slices, voxel size 0.80 × 0.80 × 0.80 mm3; and (2) 320 slices, voxel size 0.6 × 0.6 × 0.6 mm3. We adopted standard brain MR image preprocessing steps before segmentation and masked out the cerebellum and brain stem by using in-house tools [19, 20]. We should make the registration on the 7T brain MR images according to the corresponding 3T images before the manual work. Then, an expert made manual editing to correct the errors in MR image segmentation results with the tool of ITK-SNAP software [21].

2.2. Proposed Algorithm

A learning-based algorithm of brain MR images segmentation is proposed by formulating the brain segmentation as a classification with Structured Random Forest(SRF) in this paper. The SRF is very suitable for the classification problem and is applied as the classifier to produce the brain tissue probability maps. The SRF can efficiently make use of more image features to perfectly obtain local and contextual brain image information. So the segmentation consequence of brain MR image is completed based on the largest probability on each voxel location. The main novelties of the proposed method are the utilization of the 7T brain MR images to obtain the ground truth of the learning-based algorithm.

The proposed algorithm uses SRF as a supervised classifier. From (Fig. **1**), we can find that the 7T brain MR image shows excellent image intensity contrast compared with the corresponding 3T brain MR image. We find that compared with the images acquired at 3T, the 7T MR images would yield superior spatial resolution and intensity contrast. When training the random forest, we can make use of the responding 3T brain MR images attained from the dataset. So the automatic segmentation algorithm of Structured Random Forest will be trained by the 3T training sample and its ground truth.

As mentioned before, our algorithm is a supervised learning-based method. The proposed algorithm is shown in Fig. (**2**). In the training stages, a lot of classification decision trees will be trained. The key point of our algorithm is to train the SRF with the ground truth generated from the 7T image. Because the 7T brain MR images have excellent intensity contrast, the ground truth can directly and conveniently be obtained by the 7T images and show more perfect quality than the ones by using the 3T images. So there are corresponding 3T brain MR images according to the 7T images and these 3T images will be taken as the training samples to train the random forest. We have 10 training samples attained from 10 brain MR subjects.

2.3. Structured Random Forest

Random forest algorithm is a classifier with a lot of mutually independent decision trees [22-24]. RF is trained with boosting method. A RF is considered as a collection of decision trees, such as:

$$\{h(x;\psi(\mathrm{t})); \mathrm{t}=1,\cdots,\mathrm{T}\} \quad \textbf{(1)}$$

Where X is a random vector, ψ(t)are independent and identically distributed random vectors. The classification of random vector is determined by the majority voting result of mutually independent decision trees [25, 26]. The Structured Random Forest (SRF) [27] is designed to utilize the structural information for image labeling and image segmentation. In SRF, all label distributions are mapped to a discrete space at each split node in a random forest to achieve the standard information gain measures. Then, the predicted distribution can be obtained directly without calculating the probability of each class individually. SRF shows higher accuracy and lower standard deviations among different measurements.

2.4. Appearance and Context Features

In our work, the 3D Haar-like features are as follows:

$$f(x,I)=\frac{1}{R_1}\sum_{u\in R_1}I(u)-b\frac{1}{R_2}\sum_{v\in R_2}I(v), R_1\in R, R_2\in R, b\in\{0,1\} \quad \textbf{(2)}$$

Where R is the patch that centers at the voxel x, R_1 and R_2 are randomly and independently displaced cubical regions. I is the source image, and the parameter b $\in$ {0,1} indicates whether one or two cubical regions are used [28, 29].

In the training stage, a series of classification decision trees are trained. In the first iteration, only the T1-weighted images are taken as input source for voxel-wise classification. In the later iterations, we select the three tissue probability maps as additional source input images. The iteration is repeated in the training process and the tissue probability

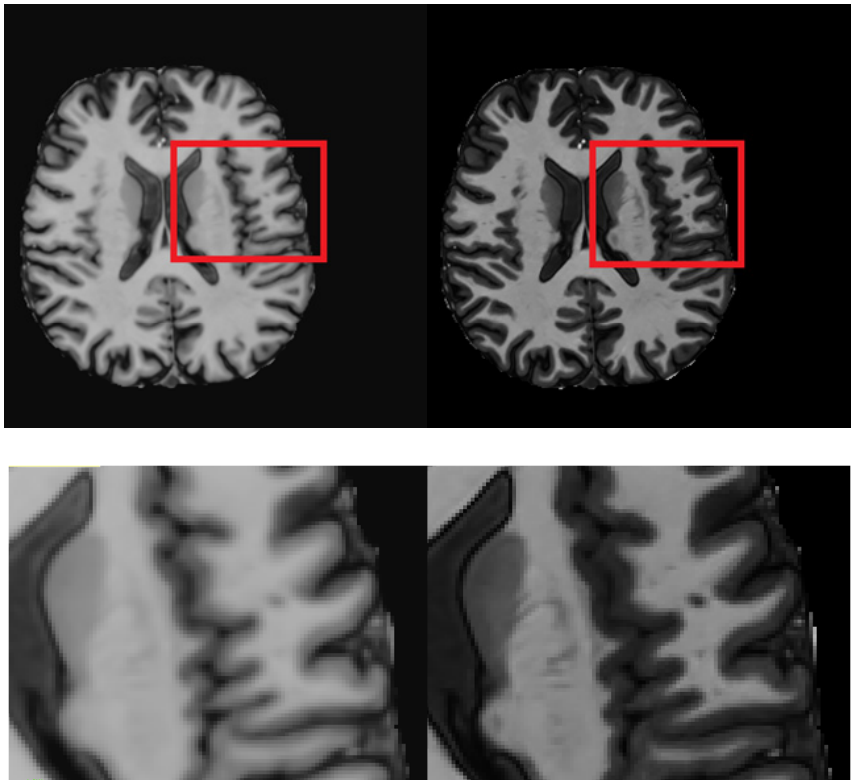

Fig. (1). The comparison of the image intensity constant between 3T brain MR image and 7T brain MR image. *(A higher resolution / colour version of this figure is available in the electronic copy of the article)*.

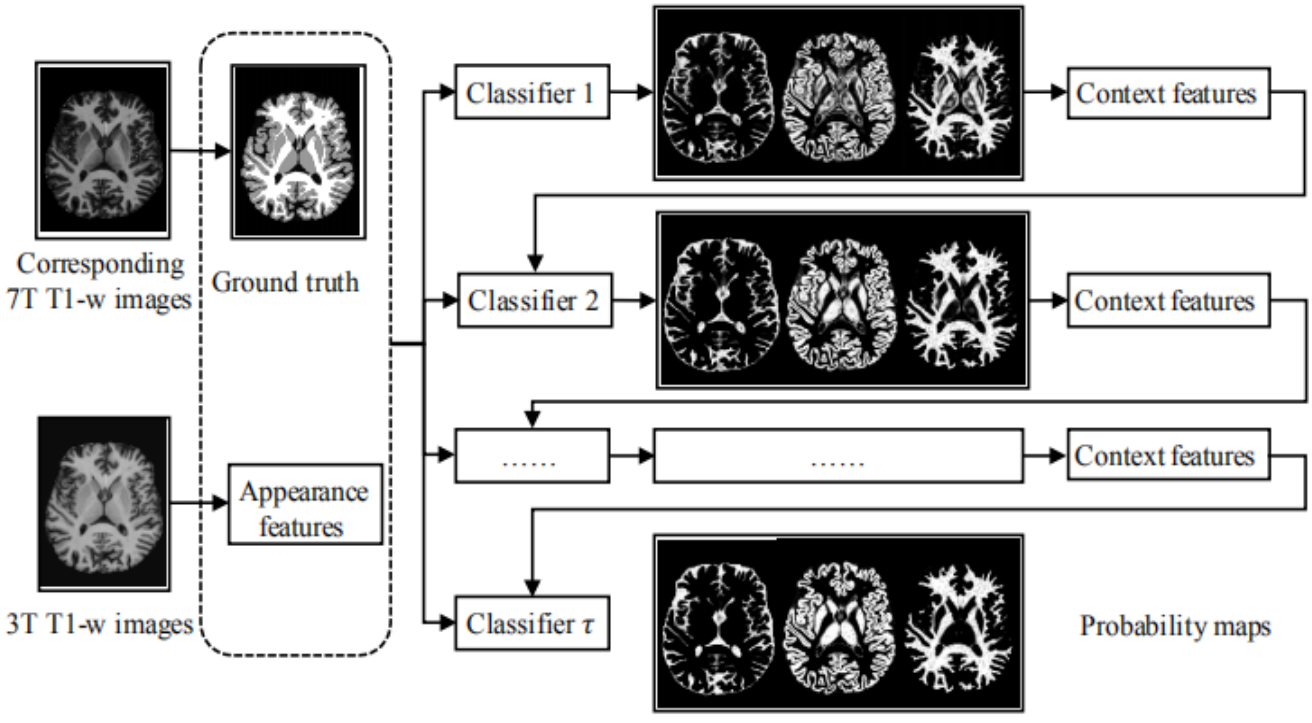

Fig. (2). Flowchart of our proposed algorithm with T1 weighed images of the three probability maps for the training of decision trees. *(A higher resolution / colour version of this figure is available in the electronic copy of the article)*.

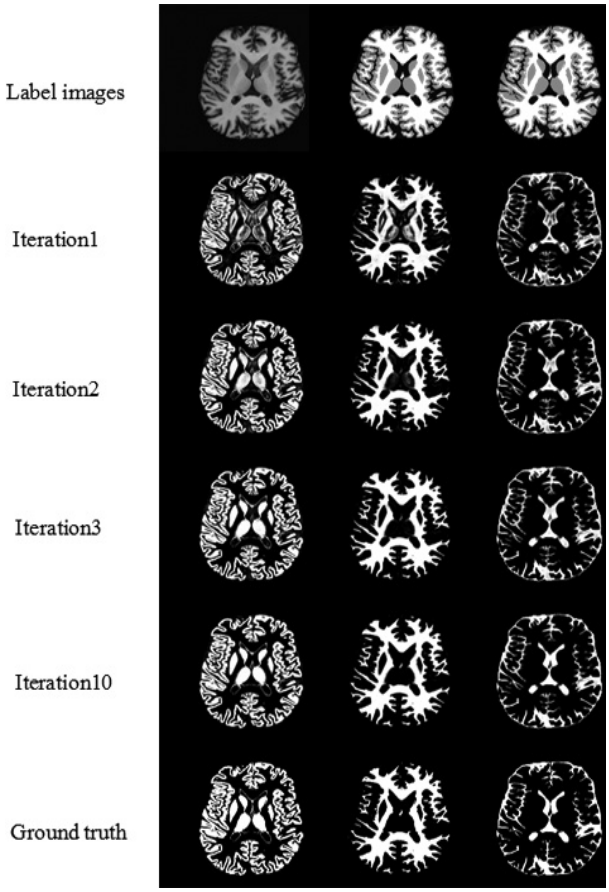

Fig. (3). The original image, consequence of proposed algorithm on Subject 6 and ground truth. The tissue probability maps of GM, WM and CSF by applying the decision trees on a target subject. *(A higher resolution / colour version of this figure is available in the electronic copy of the article)*.

maps of previous iteration will be used as supplemental sources for exact context features. In the testing stage, each voxel independently goes through each tree until the voxel arrives at a leaf. The class probability of the testing sample is determined by the average of the class probabilities of the leaf node in decision trees. In this paper, the random forest through the iteration will produce three tissue probability maps for GM, WM and CSF. Eventually, the final results of classification are obtained shown in Fig. (**3**). In (Fig. **3**), we apply trained random forest classification algorithm on a testing brain MR subject. From (Fig. **3**), we can find that the tissue probability maps are increasingly improved in the iteration. They are more and more accurate according to the ground truth. So, the brain MR subject segmentation consequences are perfect and desirable in the iteration classification procedure.

2.5. The Statistical Software and Experimental Tests

A section statistical analysis should be added at the end of materials and methods to show which statistical software and which tests were used to compare the results. In this paper, the matlab software was used to calculate the results of statistical analysis. We designed the matlab program to calculate the Dice ratio over different images achieved by the proposed algorithm, FSL, MIPAV and SPM and apply the leave-one-out cross validation on all subjects to calculate the Dice ratio with different algorithms. The segmentation results with respect to the Dice ratio of GM, WM and CSF prove the superiority of the proposed automatic scheme. Then, we compare the segmentation accuracies with Dice ratios of 7 different methods on 10 subjects in terms of Dice ratio achieved by the support vector machine (SVM), coupled level sets (CLS), majority voting (MV), Atlas forest, Nonlocal label fusion, classical random forest (RF), and proposed algorithm. In this paper, we have 10 training subjects of T1 brain images and achieve the segmentation results of tissues of GM, WM and CSF, Label difference maps of GM, WM and CSF and 3D surfaces of segmentation results with the proposed automatic segmentation scheme on the 3T brain MR images. These consequences perfectly illustrate that the proposed automatic segmentation scheme is more effective than other automatic segmentation software FSL, MIPAV, and SPM. We have made the segmentation on 797 ADNI subjects with the proposed method. And then, the segmentation on 797 ADNI subjects with the proposed method was made. Because of the lack of the ground truth of ADNI subjects, we make comparisons with FSL on the detection of group differences between AD *vs* NC, and MCI *vs* NC. The GM/WM difference between maps of AD *vs* NC, and MCI

vs NC shows the accurate and satisfactory WM cortical atrophies in the brain MRI images with our proposed algorithm.

3. RESULTS

In the implementation of our automatic segmentation algorithm, 30,000 training voxels are randomly selected in each training brain MR subject. The number of classes in the classification of random forest are 3 (GM, WM and CSF). All training images would be resampled to the image spacing of 0.65×0.65×0.65. The number of input images of random forest for classification is 1 in the first iteration and 4 in the other iterations. We devise 10 iteration processes in our training of random forest. The patch size of each training voxel is set as 9 × 9 × 9 patch. In each iteration, 20 classification trees are trained and the maximum tree depth is 100 according to the current implementation capability. The minimum sample size of each leaf node is 8 and the total number of Haar-like features generated are 10,000 in each tree. To evaluate the excellence of the proposed algorithm of 7T MR, we have also compared the following automatic medical image processing software: FSL, MIPAV, and SPM with our proposed automatic segmentation scheme in this paper and the segmentation consequences are shown in Fig. (**4**).

We apply the leave-one-out cross validation on all subjects to calculate the Dice ratio with different algorithms. The proposed automatic scheme improves the segmentation results with respect to the Dice ratio of GM, WM and CSF shown in Table **1**. The comparison between the proposed automatic scheme and FSL, MIPAV, and SPM shows that the proposed scheme outperforms other segmentation methods in the most time. Specifically, proposed automatic scheme achieved mean (± standard deviation) Dice ratios as 0.9017 ± 0.0183(GM), 0.9514 ± 0.0090(WM) and 0.8196 ± 0.0432(CSF) on average over 10 subjects, yielding an overall value of 0.8799 ± 0.0603. In contrast, FSL, MIPAV and SPM achieved overall Dice ratios of 0.7922 ± 0.1194, 0.7917 ± 0.1194, 0.7607 ± 0.0880, respectively. Consequently, the proposed automatic scheme outperformed other methods with Dice ratios.

For clearly demonstrating the advantage of the proposed automatic segmentation scheme, the segmentation results of tissues of GM, WM and CSF with subject 2 are shown in Fig. (**4**). The first column lists the original brain MR images, and the sixth column shows the corresponding results of human experts. The following four columns present the results of the proposed automatic segmentation scheme, FSL, MIPAV and SPM. We can find that the segmentation consequences is very close to the ground truth. In comparison, there are more errors and fuzzy boundaries in segmentation of FSL, MIPAV, and SPM. These consequences perfectly illustrate that the proposed automatic segmentation scheme is more effective than other methods. Label difference generated by the proposed algorithm, FSL, MIPAV and SPM on subject 7 are shown in Fig. (**5**). We can see that the proposed automatic segmentation scheme outperformed the current medical image automatic processing software FSL, MIPAV, and SPM.

We have made the segmentation on 797 ADNI subjects with the proposed method. We compare these segmentation results with other methods shown in Fig. (**6**). The first column shows original T1-weighted images and the second column shows the consequences of the proposed algorithm. The third and fourth columns show the segmentation results with FSL and MIPAV. But the segmentation on ADNI by use of the SPM is unsuccessful and is not shown in Fig. (**6**). The comparison of 3D surfaces of segmentation results with different methods is shown. The first row shows the 3D gray matter surfaces with the proposed algorithm, FSL and MIPAV and the second row shows the 3D white matter surfaces with the proposed algorithm, FSL and MIPAV. From (Fig. **7**), 3D surfaces show the advantage of the proposed algorithm. We can find that the proposed algorithm outperforms other algorithms in the performance of tissue boundary detection and shows higher accuracy of the segmentation on the boundary pixels.

The DICOM files with proposed algorithm, FSL and MIPAV have been uploaded as supporting information. Since there is no ground truth, it may be difficult to make a quantitative comparison between them in terms of Dice ratios. Alternatively, we make comparisons with FSL on the detection of group differences between AD *vs* NC, and MCI *vs* NC. We compare the GM/WM difference between maps of AD *vs* NC, and MCI *vs* NC with different algorithms. (Fig. **7**) shows the GM/WM volume differences between AD *vs* NC. Both results by our method and FSL method have shown significant cortical atrophy in the pictures. However, FSL method wrongly identified WM regions that are even larger than that of controls, which is opposite to the real case. The possible reason is that FSL method under-segmented GM or over-segmented WM, or both of them. By contrast, our algorithm showed accurate and satisfactory WM cortical atrophies in the brain MRI images.

In (Fig. **7**), group volume difference of AD *vs* NC is shown. Red is used to indicate expansion and blue is used to indicate atrophy ($p<0.05$ FDR corrected, cluster size > 50). Form the volume differences, we can conclude that our algorithm is superior to other mainstream automatic segmentation algorithms for brain MRI images. Our algorithm can give convincing and reasonable brain MRI images segmentation results.

Our current experiments are implemented on a computer cluster (3.3 GHz Intel processors, 12 M L3 cache, and 64 GB memory). There are total 6 iterations, and, for each iteration, 20 trees are trained. All trees in each iteration are trained in a parallel way and the average training time for one tree is about 1.5 hours, thus the total training time is around 1.5 h×6 iterations =9h. For testing on a typical 3T brain MR image, the average runtime is about 10 mins.

4. DISCUSSION

We compared our method with other segmentation methods provided in the following software packages: FSL, Medical Image Processing, Analysis and Visualization (MIPAV) and Statistical Parametric Mapping (SPM). The leave-one-

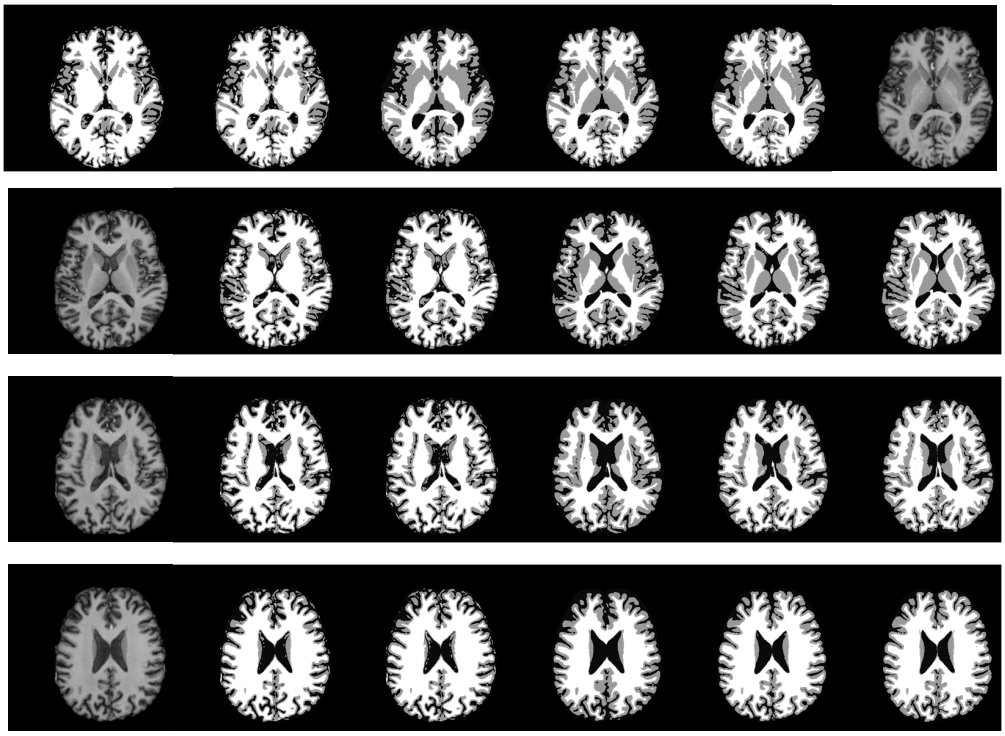

(a) Original image (b)FSL (c) MIPAV (d) SPM (e) Proposed (f)Ground truth

Fig. (4). (**a-f**) Comparison segmentation results over Subject 2. The first column shows the four slices of original T1 weighted image. The second, third, fourth and fifth columns show the segmentation results with FSL, MIPAV, SPM and proposed algorithm. *(A higher resolution / colour version of this figure is available in the electronic copy of the article)*.

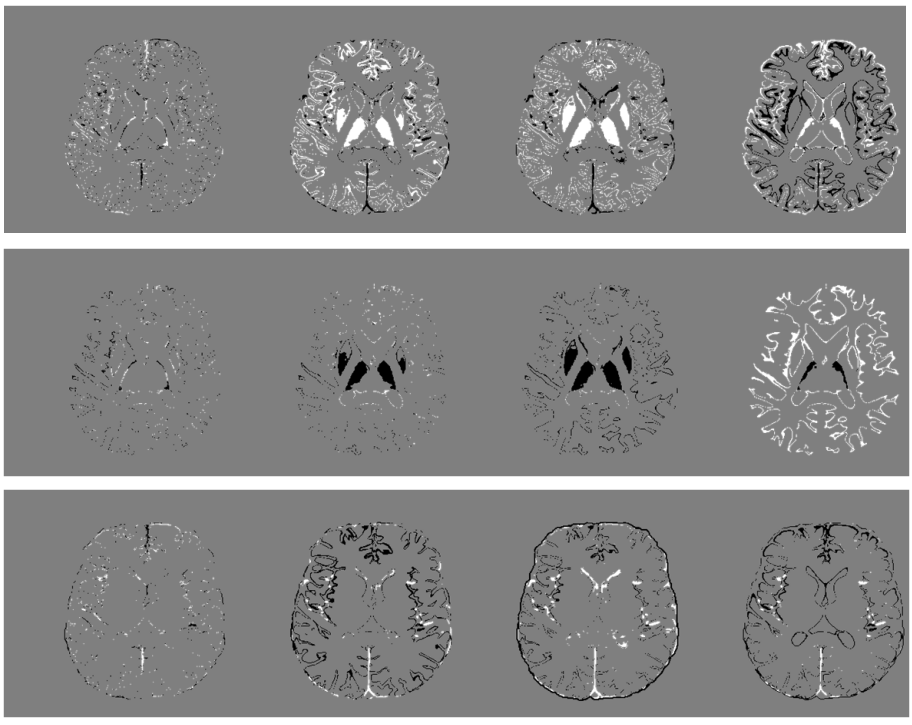

(a) Proposed (b) FSL (c) MIPAV (d) SPM

Fig. (5). (**a-d**) Label difference maps generated by proposed algorithm, FSL, MIPAV and SPM on subject 7. *(A higher resolution / colour version of this figure is available in the electronic copy of the article)*.

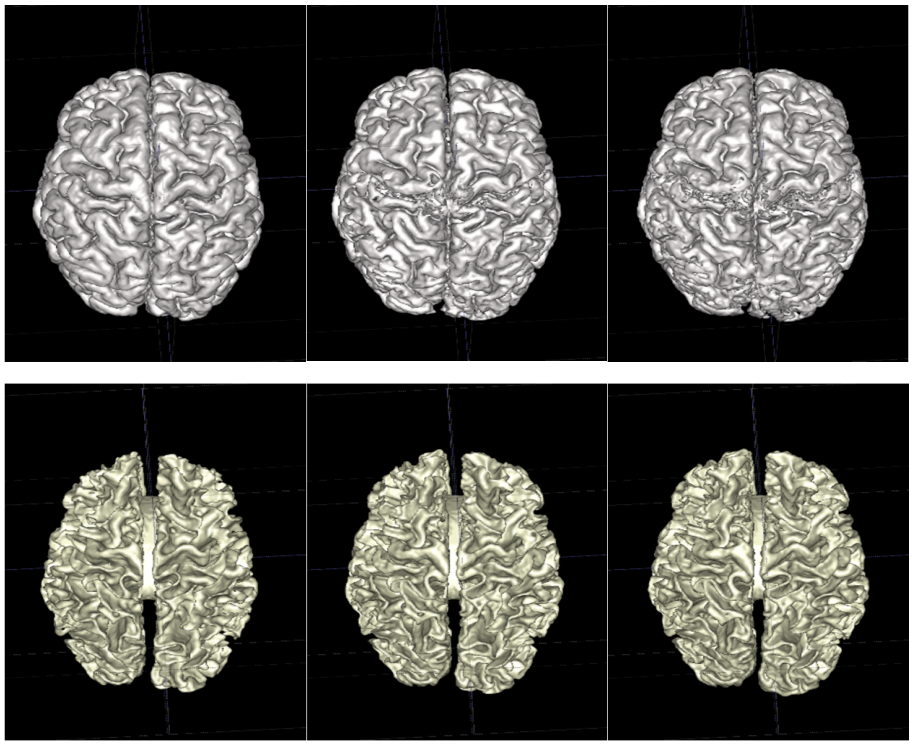

(a) Proposed (b) FSL (c) MIPAV

Fig. (6). (**a-c**) Comparison of 3D surfaces of segmentation results. The first row shows the 3D gray matter surfaces with proposed algorithm, FSL and MIPAV. The second row shows the 3D white matter surfaces with the proposed algorithm, FSL and MIPAV. *(A higher resolution / colour version of this figure is available in the electronic copy of the article)*.

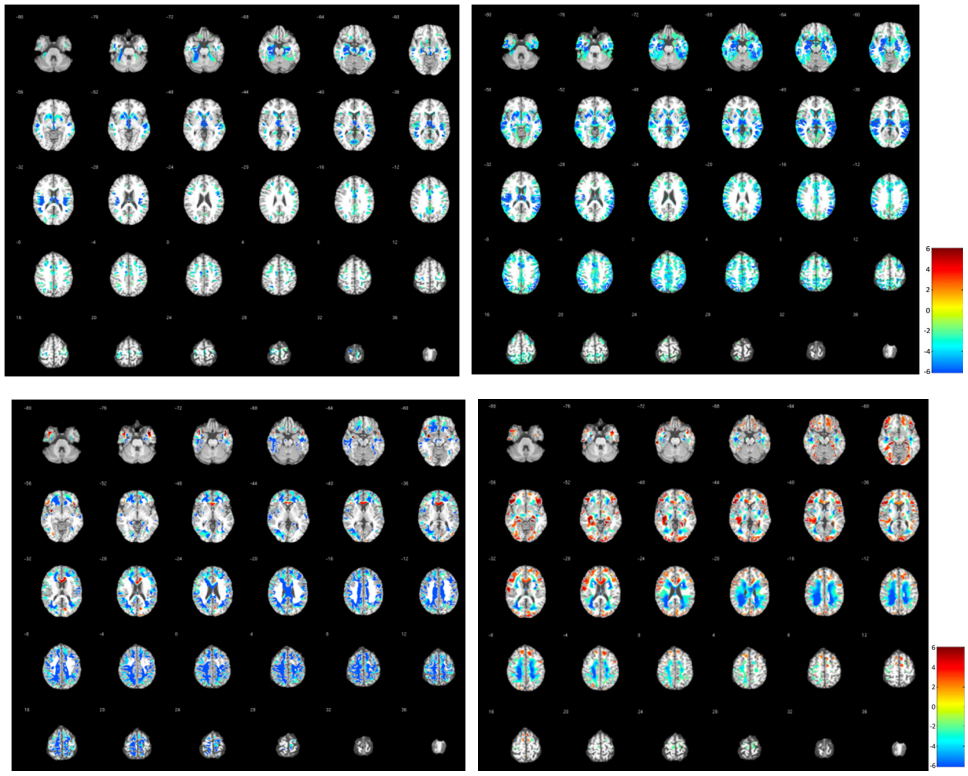

Fig. (7). Group volume difference of AD *vs* NC by the proposed method and FSL method. *(A higher resolution / colour version of this figure is available in the electronic copy of the article)*.

Table 1. Comparison of Dice ratio over different images achieved by the proposed algorithm, FSL, MIPAV and SPM.

Dice Ratio		Sub.1	Sub.2	Sub.3	Sub.4	Sub.5	Sub.6	Sub.7	Sub.8	Sub.9	Sub.10	Mean
GM	Proposed	**0.8787**	**0.8980**	**0.8958**	**0.8998**	**0.8861**	**0.9258**	**0.9092**	**0.9046**	**0.9130**	**0.9055**	**0.9017±0.0183**
	FSL	0.8339	0.8185	0.8132	0.8309	0.8103	0.8107	0.7875	0.8307	0.8213	0.7757	0.8133±0.0180
	MIPAV	0.8431	0.8174	0.8166	0.8056	0.8192	0.8389	0.7970	0.8447	0.8343	0.8385	0.8255±0.0158
	SPM	0.7739	0.7758	0.7971	0.7775	0.7953	0.7881	0.796	0.7801	0.8463	0.7021	0.7832±0.0336
WM	Proposed	**0.9467**	**0.9522**	**0.9494**	**0.9496**	**0.9447**	**0.9592**	**0.9520**	0.9445	**0.9570**	**0.9590**	**0.9514±0.0090**
	FSL	0.9415	0.8796	0.8860	0.8998	0.8517	0.9529	0.9013	**0.9500**	0.9276	0.9587	0.9149±0.0346
	MIPAV	0.9282	0.8749	0.8869	0.8685	0.8676	0.9232	0.9033	0.9437	0.9202	0.9490	0.9066±0.0291
	SPM	0.8208	0.7978	0.8141	0.8125	0.8026	0.8321	0.873	0.8346	0.8482	0.8422	0.8278±0.0218
CSF	Proposed	**0.8210**	**0.8321**	**0.7801**	**0.8394**	**0.7535**	**0.8848**	**0.8632**	**0.8170**	**0.7762**	**0.8291**	**0.8196±0.0432**
	FSL	0.6479	0.6046	0.6075	0.6312	0.4970	0.7748	0.6973	0.6494	0.6629	0.7072	0.6480±0.0699
	MIPAV	0.6469	0.5965	0.5989	0.6151	0.4834	0.7514	0.6967	0.7075	0.6380	0.6959	0.6430±0.0721
	SPM	0.6777	0.6332	0.5176	0.6970	0.5190	0.7832	0.7343	0.7783	0.7515	0.6191	0.6711±0.0928

Table 2. Segmentation performance in terms of Dice ratio achieved by the support vector machine (SVM), coupled level sets (CLS), majority voting (MV), Atlas forest, Nonlocal label fusion, classical random forest (RF), and proposed algorithm.

Dice Ratio	SVM	CLS	MV	Atlas	Nonlocal Label Fusion	RF	Proposed
GM	0.8038±00690	0.8421±0.0740	0.0849±0.0101	0.0871±0.0076	0.0871±0.0076	0.8930±0.0057	0.9017±0.0183
WM	0.8172±0105	0.8297±0.0830	0.0825±0.0105	0.0889±0.6000	0.0890±0.0074	0.9112±0.0142	0.9514±0.0090
CSF	0.7333±0369	0.8038±0169	0.0806±0.0155	0.0804±0.0217	0.0801±0.0110	0.8263±0.0110	0.8196±0.0432

out cross-validation based Dice ratios for the 10 training subjects. The results indicate that the proposed method outperforms other methods for all three tissue types in most cases. Specifically, for the average Dice ratio of all 10 subjects, our method performs much better than any other comparison methods. For example, compared to the best method, our method improves about 8% for GM, > 4% for WM, and > 17% for CSF. Qualitative results for visual inspection are also shown in Fig. (**4**) to Fig. (**6**).

From the experiments, our method, compared with FSL, MIPAV and SPM, could produce perfect results that are significantly consistent with the ground truth segmentations. The WM surfaces generated by the ground truth and different methods show the differences of the label maps with respect to the ground-truth segmentations and indicates that the proposed method produces better segmentation with less false positives and false negatives compared with commonly used state of the art brain MRI automatic segmentation methods.

In order to demonstrate the effectiveness and superiority of the proposed algorithm, we compare the segmentation accuracies with Dice ratios of 7 different methods on 10 subjects. Segmentation performances in terms of Dice ratio achieved by the support vector machine (SVM), coupled level sets (CLS), majority voting (MV), Atlas forest, Nonlocal label fusion, classical random forest (RF), and proposed algorithm are shown in Table **2**. The segmentation performances denote that the proposed algorithm is superior to the other 6 learning-based algorithms in the accuracy of segmentation in most cases, on average over 10 subjects. It can be observed that the segmentation results of tissues of GM and WM with the proposed algorithm yielded higher performance than any of other 6 learning-based methods. This suggests that the proposed method can achieve promising results with the least computational errors. These results demonstrate that 7T learning-based algorithm is more informative in distinguishing certain tissue types, and leads to improved segmentation performance.

CONCLUSION

In this paper, the segmentation problem of 3T brain images was transformed into a patch classification question for the classifiers of the structured random forest with the ground truth directly obtained from the corresponding 7T brain MR images. Our algorithm achieved the segmentation of three tissue probability maps for GM, WM and CSF. For comparison purposes, we also implemented six commonly used segmentation algorithm, such as the support vector machine (SVM), coupled level sets (CLS), majority voting (MV), Atlas forest, Nonlocal label fusion and classical random forest (RF). The support vector machine (SVM) (Burges, 1998) [30] are inherently binary classifiers. In order to make the segmentation on the MR brain image and achieve classifying tissues of the brain, they are often applied hierarchically or in the one-versus-all manner. Usually, several different classes have to be grouped together, which may make the classification task more complex than it should be. The performance of support vector machine (SVM) are generated by tuning the regularization parameters using cross validation. The classical RF is a tree-based ensemble model in which a set of randomized trees are built and the final decision is made using majority voting by all trees. This method has been used in MR image segmentation (Criminisi and Shotton, 2013; Criminisi, *et al.*, 2012) [31,

32]. The coupled level set (CLS) (Wang *et al.*, 2011) [33] is designed to combine the local intensity information, atlas spatial prior, and cortical thickness constraint in a level-set framework. The majority voting (MV) methods (Wang *et al.*, 2014) [13] require the images of different subjects to be registered, since a local dictionary was constructed by using patches extracted from the corresponding locations on the training images. The atlas-based methods are proposed for the automatic segmentation of brain MR image. A new atlas framework is designed for performing neonatal brain tissues segmentation by using a subject-specific tissue probabilistic atlas generated from the follow-up data of the same subject (Kuklisova-Murgasova *et al.*, 2011) [34]. The novel patch-based method is proposed for automatic extraction of anatomical structures by using the expert manual segmentation as priors. By taking advantages of the redundancy of information present in the image, the patch-based non-local means scheme enables the robust use of a large number of samples during estimation. A patch-based weight is used to perform a pixel-based aggression of the labels ensuring the independence of the votes (Coupé, P., *et al.*, 2011) [35]. The performance of SVM, CLS, MV, Atlas, Nonlocal label fusion, RF and proposed algorithm was reported in Table **2** with the Dice ratio. It can be observed that our proposed algorithm outperformed other methods for the segmentation of brain tissues in most cases. Specifically, our proposed algorithm could achieve Dice ratios as 81.96%±4.32% (CSF), 90.17%±1.83% (GM), and 95.14±0.90% (WM) on average over 10 subjects. In contrast, SVM, CLS, MV, Atlas, Nonlocal label fusion and RF achieved the overall best Dice ratios of 82.63±1.10%, 89.30±5.57%, 91.12±1.42%, respectively. After all, our proposed algorithm outperformed other methods in terms of segmentation of brain MR images.

In this paper, we aimed at segmenting the 3T brain tissues based on Structured Random Forest. We presented a learning-based automatic segmentation algorithm by effectively making use of the 7T MR images and employing the classifiers of Structured Random Forest. The learning-based automatic segmentation algorithm could combine the T1-weighted images with the tentatively estimated tissue probability maps. Firstly, we trained the classifiers of Structured Random Forest with the 3T brain MR images and corresponding ground truth obtained from 7T MR images. Then, in the next classification stage, the proposed automatic segmentation algorithm could integrate the T1-weighted images and the probability maps of GM, WM and CSF estimated in the last iteration. We compare the performances of our approach with those of the commonly used automatic segmentation methods such as FSL, MIPAV, and SPM. Results showed that our proposed automatic segmentation algorithm significantly outperformed other states of the art methods on brain MR tissue segmentation.

In our work, the brain tissue segmentation problem was transformed into a patch classification task for the classifiers of the random forest. In our proposed automatic segmentation algorithm, the classifiers of Structured Random Forest are trained with the ground truth directly obtained from the corresponding 7T brain MR images. We employed the classifiers of Structured Random Forest iteratively trained with the input of multi-source images such as T1-weighted images and tissue probability maps of WM, GM and CSF from the previous classification. The studies showed that the classifiers of the random forest yield very promising performance on brain MR tissue automatic segmentation compared with the support vector machine (SVM), coupled level sets (CLS), majority voting (MV), Atlas forest, Nonlocal label fusion and classical random forest (RF). Further experiments were performed on the 3T brain MR images of ADNI dataset and the proposed method shows excellent performances. The performance of our proposed automatic segmentation algorithm outperformed other state of the art methods on brain MR tissue segmentation and the segmentation performances of three brain tissues were balanced and stable. In the future, we will explore new intelligent automatic segmentation algorithm. But still, brain MRI segmentation is a challenging task and there is a need for future research to improve the accuracy, precision and speed of segmentation methods.

ETHICS APPROVAL AND CONSENT TO PARTICIPATE

This study was approved by the Institutional Review Board (IRB) of the Northeast Agricultural University, China (07020200352).

HUMAN AND ANIMAL RIGHTS

No animals were used in this research. All human research procedures were followed in accordance with the ethical standards of the committee responsible for human experimentation (institutional and national), and with the Helsinki Declaration of 1975, as revised in 2013.

CONSENT FOR PUBLICATION

Written informed consent forms were obtained from all subjects.

AVAILABILITY OF DATA AND MATERIALS

Not applicable.

FUNDING

This paper is supported by Harbin Science and Technology Innovation Talent Project (NO.2017RQXJ079).

CONFLICT OF INTEREST

The authors of this manuscript declare no relationships with any companies whose products or services may be related to the subject matter of the article.

ACKNOWLEDGEMENTS

Grateful acknowledgement is made to my wife Mrs. Jingbo Zhen who gave me considerable help by means of suggestion, comments and criticism. Her encouragement and unwavering support has sustained me through frustration and depression. Without her pushing me ahead, the completion of this thesis would be impossible. In addition, I deeply appreciate the contribution to this thesis made in various ways by my friends.

REFERENCES

[1] Benoit Caldairou N, Piotr A. Habas, ColinStudholme, Francois Rousseau. A non-local fuzzy segmentation method: Application to brain MRI. Pattern Recognit 2011; 44: 12.

[2] Han X, Fischl B. Atlas renormalization for improved brain MR image segmentation across scanner platforms. IEEE Trans Med Imaging 2007; 26(4): 479-86. http://dx.doi.org/10.1109/TMI.2007.893282 PMID: 17427735

[3] Chen Y, Zhao B, Zhang J, Zheng Y. Automatic segmentation for brain MR images *via* a convex optimized segmentation and bias field correction coupled model. Magn Reson Imaging 2014; 32(7): 941-55. http://dx.doi.org/10.1016/j.mri.2014.05.003 PMID: 24832358

[4] Morra JH, Tu Z, Apostolova LG, Green AE, Toga AW, Thompson PM. Comparison of AdaBoost and support vector machines for detecting Alzheimer's disease through automated hippocampal segmentation. IEEE Trans Med Imaging 2010; 29(1): 30-43. http://dx.doi.org/10.1109/TMI.2009.2021941 PMID: 19457748

[5] Powell S, Magnotta VA, Johnson H, Jammalamadaka VK, Pierson R, Andreasen NC. Registration and machine learning-based automated segmentation of subcortical and cerebellar brain structures. Neuroimage 2008; 39(1): 238-47. http://dx.doi.org/10.1016/j.neuroimage.2007.05.063 PMID: 17904870

[6] Pitiot A, Delingette H, Thompson PM, Ayache N. Expert knowledge-guided segmentation system for brain MRI. Neuroimage 2004; 23(Suppl. 1): S85-96. http://dx.doi.org/10.1016/j.neuroimage.2004.07.040 PMID: 15501103

[7] Golland P, Grimson WE, Shenton ME, Kikinis R. Detection and analysis of statistical differences in anatomical shape. Med Image Anal 2005; 9(1): 69-86. http://dx.doi.org/10.1016/j.media.2004.07.003 PMID: 15581813

[8] Zhang W, Li R, Deng H, *et al.* Deep convolutional neural networks for multi-modality isointense infant brain image segmentation. Neuroimage 2015; 108: 214-24. http://dx.doi.org/10.1016/j.neuroimage.2014.12.061 PMID: 25562829

[9] Kim EY. Machine-learning based automated segmentation tool development for large-scale multicenter MRI data analysis. Dissertations of University of Iowa 2013. http://dx.doi.org/10.17077/etd.u5b4jszi

[10] Amod Jog SR, Jerry L. Prince, Aaron Carass. Brain MR Segmentation using Decision Trees. MRBrains 2013; 13: 9.

[11] Sérgio Pereira JF. José António Mariz, Nuno Sousa, *et al.* Automatic Brain Tissue Segmentation of Multi-sequence MR images using Random Decision Forests. Proceedings of NCI-MICCAI BRATS. 6

[12] Mitra J, Bourgeat P, Fripp J, *et al.* Lesion segmentation from multimodal MRI using random forest following ischemic stroke. Neuroimage 2014; 98: 324-35. http://dx.doi.org/10.1016/j.neuroimage.2014.04.056 PMID: 24793830

[13] Wang L, Shi F, Gao Y, *et al.* Integration of sparse multi-modality representation and anatomical constraint for isointense infant brain MR image segmentation. Neuroimage 2014; 89: 152-64. http://dx.doi.org/10.1016/j.neuroimage.2013.11.040 PMID: 24291615

[14] Beisteiner R, Robinson S, Wurnig M, *et al.* Clinical fMRI: evidence for a 7T benefit over 3T. Neuroimage 2011; 57(3): 1015-21. http://dx.doi.org/10.1016/j.neuroimage.2011.05.010 PMID: 21620980

[15] Bernstein MA, Huston J III, Ward HA. Imaging artifacts at 3.0T. J Magn Reson Imaging 2006; 24(4): 735-46. http://dx.doi.org/10.1002/jmri.20698 PMID: 16958057

[16] Hahn A, Kranz GS, Seidel EM, *et al.* Comparing neural response to painful electrical stimulation with functional MRI at 3 and 7 T. Neuroimage 2013; 82: 336-43. http://dx.doi.org/10.1016/j.neuroimage.2013.06.010 PMID: 23769917

[17] Sladky R, Baldinger P, Kranz GS, *et al.* High-resolution functional MRI of the human amygdala at 7 T. Eur J Radiol 2013; 82(5): 728-33. http://dx.doi.org/10.1016/j.ejrad.2011.09.025 PMID: 22138120

[18] Braun J, Guo J, Lützkendorf R, *et al.* High-resolution mechanical imaging of the human brain by three-dimensional multifrequency magnetic resonance elastography at 7T. Neuroimage 2014; 90: 308-14. http://dx.doi.org/10.1016/j.neuroimage.2013.12.032 PMID: 24368262

[19] Shi F, Wang L, Dai Y, Gilmore JH, Lin W, Shen D. LABEL: pediatric brain extraction using learning-based meta-algorithm. Neuroimage 2012; 62(3): 1975-86. http://dx.doi.org/10.1016/j.neuroimage.2012.05.042 PMID: 22634859

[20] Sled JG, Zijdenbos AP, Evans AC. A nonparametric method for automatic correction of intensity nonuniformity in MRI data. IEEE Trans Med Imaging 1998; 17(1): 87-97. http://dx.doi.org/10.1109/42.668698 PMID: 9617910

[21] Yushkevich PA, Piven J, Hazlett HC, *et al.* User-guided 3D active contour segmentation of anatomical structures: significantly improved efficiency and reliability. Neuroimage 2006; 31(3): 1116-28. http://dx.doi.org/10.1016/j.neuroimage.2006.01.015 PMID: 16545965

[22] Amit Y, Geman D. Shape quantization and recognition with randomized trees. Neural Comput 1991; 9(7): 43.

[23] Breiman L. Bagging predictors. Mach Learn 1996; 24(2): 18. http://dx.doi.org/10.1007/BF00058655

[24] Ho T. The random subspace method for constructing decision forests. IEEE Trans Pattern Anal Mach Intell 1998; 20(8): 13.

[25] Josu Maiora BA. Manuel Graña. Random forest active learning for AAA thrombus segmentation in computed tomography angiography images. Neurocomputing 2014; 126: 8.

[26] Adriano Pinto SP, Hugo Dinis, Carlos A Silva. Random decision forests for automatic brain tumor segmentation on multi-modal MRI images. IEEE 4th Portuguese BioEngineering Meeting Porto: 3 Portugal, 2015.

[27] Kontschieder P, Bulo S, Bischof H, *et al.* Structured class-labels in random forests for semantic image labelling. 2011. http://dx.doi.org/10.1109/ICCV.2011.6126496

[28] Cheng H, Liu Z, Yang L. Sparsity induced similaritymeasure for label propagation.

[29] Wright J, Yang AY, Ganesh A, Sastry SS, Ma Y. Robust face recognition *via* sparse representation. IEEE Trans Pattern Anal Mach Intell 2009; 31(2): 210-27. http://dx.doi.org/10.1109/TPAMI.2008.79 PMID: 19110489

[30] Burges CC. A tutorial on support vector machines for pattern recognition. Data Min Knowl Discov 1998; 2: 121-67. http://dx.doi.org/10.1023/A:1009715923555

[31] Criminisi A, Shotton J. Decision Forests for Computer Vision and Medical Image Analysis. Springer 2013. http://dx.doi.org/10.1007/978-1-4471-4929-3

[32] Criminisi A, Shotton J, Konukoglu E. Decision forests: a unified framework for classification, regression, density estimation, manifold learning and semi-supervised learning. Found Trends Comput Graph Vis 2012; 7(2-3): 81-227.

[33] Wang L, Shi F, Lin W, Gilmore JH, Shen D. Automatic segmentation of neonatal images using convex optimization and coupled level sets. Neuroimage 2011; 58(3): 805-17. http://dx.doi.org/10.1016/j.neuroimage.2011.06.064 PMID: 21763443

[34] Kuklisova-Murgasova M, Aljabar P, Srinivasan L, *et al.* A dynamic 4D probabilistic atlas of the developing brain. Neuroimage 2011; 54(4): 2750-63. http://dx.doi.org/10.1016/j.neuroimage.2010.10.019 PMID: 20969966

[35] Coupé P, Manjón JV, Fonov V, Pruessner J, Robles M, Collins DL. Patch-based segmentation using expert priors: application to hippocampus and ventricle segmentation. Neuroimage 2011; 54(2): 940-54. http://dx.doi.org/10.1016/j.neuroimage.2010.09.018 PMID: 20851199